IEEE Photonics Journal
An IEEE Photonics Society Publication

Open Access

Spatially Adaptive Column Fixed-Pattern Noise Correction in Infrared Imaging System Using 1D Horizontal Differential Statistics

Volume 9, Number 5, October 2017

Yanpeng Cao, ***Member, IEEE***
Zewei He
Jiangxin Yang
Yanlong Cao
Michael Ying Yang, ***Senior Member, IEEE***

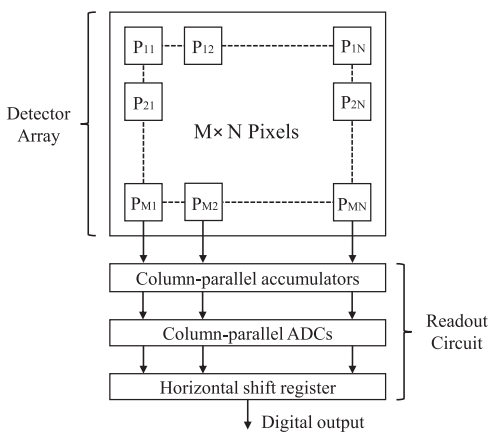

(a)

(b)

DOI: 10.1109/JPHOT.2017.2752000
1943-0655 © 2017 IEEE

Spatially Adaptive Column Fixed-Pattern Noise Correction in Infrared Imaging System Using 1D Horizontal Differential Statistics

Yanpeng Cao,[1, 2] *Member, IEEE*, Zewei He,[1, 2] Jiangxin Yang,[1, 2] Yanlong Cao,[1, 2] and Michael Ying Yang,[3] *Senior Member, IEEE*

[1]State Key Laboratory of Fluid Power Transmission and Control, School of Mechanical Engineering, Zhejiang University, Hangzhou 310027, China (e-mail: caoyp@zju.edu.cn; zeweihe@zju.edu.cn; yangjx@zju.edu.cn; sdcaoyl@zju.edu.cn)
[2]Key Laboratory of Advanced Manufacturing Technology of Zhejiang Province, School of Mechanical Engineering, Zhejiang University, Hangzhou 310027, China
[3]Scene Understanding Group, ITC, Universiteit Twente, 3230 Enschede, Overijssel Netherlands (e-mail: michael.yang@utwente.nl)

DOI:10.1109/JPHOT.2017.2752000

Manuscript received June 13, 2017; revised August 24, 2017; accepted August 25, 2017. Date of publication September 13, 2017; date of current version October 9, 2017. This work was supported in part by the National Natural Science Foundation of China under Grants 51605428, 51575486, and U1664264, and in part by the Fundamental Research Funds for the Central Universities. Corresponding author: Jiangxin Yang (e-mail: yangjx@zju.edu.cn).

Abstract: In this paper we present a novel non-uniformity correction (NUC) method to remove column fixed-pattern noise (FPN), which is introduced by non-uniformity of on-chip column-parallel readout circuit in uncooled infrared focal plane array. We first define a new image statistic measurement, which is named as 1D horizontal differential statistics, to differentiate column FPN from structural edges, and further propose a filtering scheme to adaptively compute noise terms in structure and non-structure regions by applying different correction models. The proposed NUC technique combines the advantages of global- and local-based correction methods, thus can effectively eliminate column FPN without losing original thermal details. The performance of the proposed method is systematically evaluated, and is compared with the state-of-the-art column FPN correction solutions using realistic infrared images.

Index Terms: Non-uniformity correction, focal plane array, fixed-pattern noise correction, infrared detector, infrared statistics, noise in imaging systems.

1. Introduction

Uncooled Long-Wave Infrared Focal Plane Array (FPA) typically consists of a detector array, column-parallel accumulators and analog-to-digital converters (ADCs) as depicted in Fig. 1(a) [1]. Characteristics of accumulators and ADCs in different columns are slightly changed, and such non-uniformity of readout circuit will generate column FPN. Without proper noise compensation, column FPN will appear as obvious vertical strips in a raw infrared image as shown in Fig. 1(b). The existence of column fixed-pattern noise (FPN) significantly degrades radiometric accuracy of captured infrared data and leads to performance decrease of subsequent infrared imaging applications such as

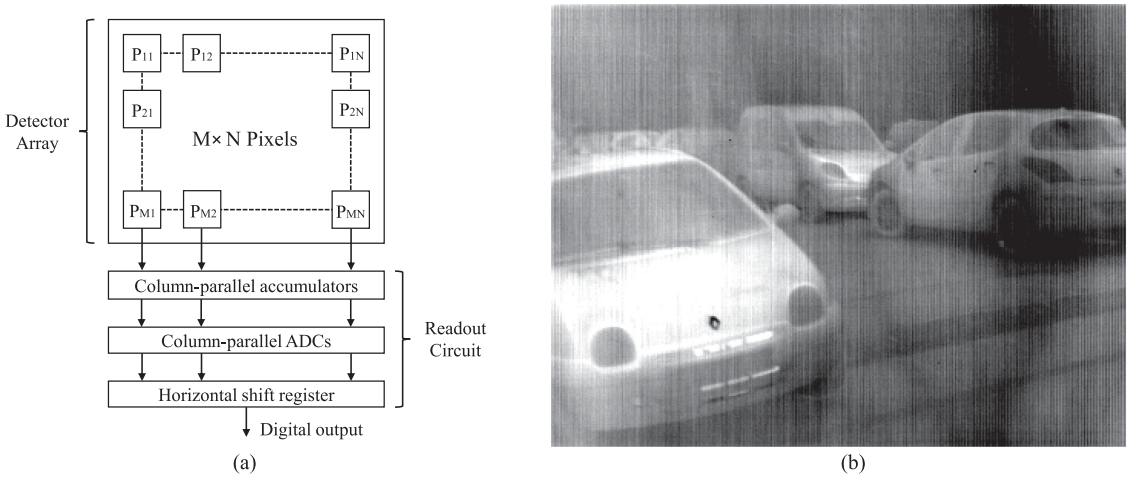

Fig. 1. Column-parallel accumulators and ADCs in infrared FPA have different characteristics and such non-uniformity of readout circuit will generate column FPN. (a) Block diagram of Uncooled Long-Wave infrared FPA. (b) A raw infrared image which contains obvious column FPN (The image is available under the Creative Commons Attribution (CC-BY) license [3]).

object recognition, thermal diagnosis, and target tracking. Moreover, strip non-uniformity cannot be properly handled by conventional Non-uniformity Correction (NUC) techniques which are developed to compensate slowly drifted spatial non-uniformity of photodetectors [2].

Although a large number of NUC methods have been reported over the past few years, it still remains a difficult problem to develop a column FPN correction method which can effectively suppress strip noise while preserving thermal details. The major challenge is two-fold. Firstly, the separation of column FPN and other high-frequency signals (e.g., image edges and textures) is difficult since their caused spatial variations are unavoidably mixed and overlapped. The underlying principle of edge-preserving filtering [4], [5] is that image edges are more significant than noise such that a threshold parameter can be set to differentiate them. However this basic assumption does not hold valid for low-contrast infrared images as strip noise sometimes is more obvious than weak image structures/textures [6]. How to remove high-variance image noise without losing low-variance true signals is a challenging task. Secondly, it is not a trivial task to develop a reference-free method to evaluate performance of strip NUC methods. Peak signal-to-noise ratio (PSNR) is commonly used as a quality measurement of denoising algorithms. A global image sharpness parameter β is proposed to determine the degree of smoothing in the denoising results [7]. However, both methods require a ground truth reference which is not available in infrared pre-processing steps (e.g., NUC). Existing reference-free evaluation metrics, such as roughness index [8], [9], Root Mean-Square Error between horizontally adjacent pixels ($RMSE_{AP}$) [10], and Energy of Line Gradient [11], can only characterize how well an algorithm can suppress high-frequency noise, but cannot indicate whether the algorithm has the ability to keep image structures and other original information. Without a proper evaluation method, it is difficult to make a good balance between noise suppression and detail preservation.

To address the above mentioned problems, we firstly propose a new NUC method which can effectively remove column FPN and further present a reference-free evaluation method. It is observed that a structural edge usually introduces local gradients of consistent orientations, while column FPN exhibits repetitive patterns in the horizontal direction and generates local variances of similar magnitudes but in different directions. With this important finding, we define a novel image statistic measurement, which is termed as 1D Horizontal Differential Statistics, to depict local image variation patterns. 1D Horizontal Differential Statistics are able to capture the essential difference between column FPN and structural edges, thus provide an effective tool to extract structure information from raw infrared images which contain obvious strip noise. Based on the computed

image structure map, a spatially adaptive filtering scheme is presented to compute noise terms in structure and non-structure regions individually by applying different correction models, therefore it can effectively eliminate column FPN while preserving other high-frequency signals including major edges and image details. Moreover, we present a reference-free methodology to investigate how horizontal gradient suppression is differently performed in structure and non-structure regions. The calculated results can be used not only to assess how well an algorithm removes column FPN but also to depict its ability to preserve image details.

The remainder of the paper is organized as follows. Related works are reviewed in Section 2. The details of our proposed column FPN correction method are given in Section 3. A new reference-free NUC evaluation method is presented in Section 4. In Section 5 our proposed noise removal method is compared with existing state-of-the-art solutions. Finally, the conclusions are given in Section 6.

2. Related Works

The most commonly used NUC technique is based on radiometric calibration. For example, through a calibration procedure known as "two-point method" or "shutter-based correction", an array of individual correction factors (gain and offset) are computed and further applied to each corresponding pixels in raw image to eliminate spatial non-uniformity of FPA [12]. However, the requirement for an internal shutter will increase the size, weight, power and manufacturing cost of an infrared imaging system. Moreover, real-time image capturing will be interrupted for a few seconds every time when a calibration procedure is performed. To overcome the above limitations, numerous shutterless NUC approaches have been proposed based on scene tracking and temporal filtering [13]–[18]. A major limitation of scene-based NUC algorithms is that they usually need to store and process a number of image frames to estimate stable correction factors. This requirement makes their real-time hardware implementation difficult. Moreover, the performance of scene-based NUC algorithms is highly dependent on the amount of object motion in the image sequence. If an image sequence does not contain enough scene motions, objects in previous images may appear as the accumulated "ghosting" artifacts in the current frame [19]. Recently, a number of single-image based NUC methods have been proposed to overcome the above limitations [10], [19]–[21].

Infrared images typically contain a limited amount of edges/textures information [6]. Important targets will no longer be detected/recognized if the low-contrast infrared images are over-smoothed. How to effectively remove FPN in infrared images without losing original information is a challenging task. Experimental results indicate that general 2D denoising filters (e.g., guided filter [22], non-local means [23], BM3D [24]), which work well for visible images, are not suitable to process low-textured infrared images and will falsely remove valuable thermal details [10]. Recently, a number of studies have been performed on removing strip non-uniformity presented in individual columns. In low-contrast infrared images, column FPN sometimes is more significant than weak image structures/textures, therefore strong strips will remain while weak edges get removed by setting a fixed threshold [11], [25]. Narayanan *et al.* firstly grouped pixels from the same readout channel (e.g., within a column) and applied a linear correction model to normalize outputs of these channels [19]. Based on column Midway Histogram Equalization, Tendero *et al.* proposed NUC methods which can effectively eliminate strip FPN without blurring edges [3], [26]. However, MHE algorithm is not capable of removing significant column FPN and sometimes generates undesired image artifacts. Cao *et al.* made use of local 1D guided filters, which can be efficiently implemented in FPGA processor, to remove significant strip noise without blurring important image details or causing undesired artifacts [10]. However this method applied fixed-size filters to separate strip noise from other high-frequency signals and will blur long vertical edges in infrared images. Chang *et al.* proposed a variational strip removal algorithm that combines unidirectional total variation and framelet regularization [27]. However, such optimization-based methods are not easily accelerated in the form of filter due to the need of solving large linear systems [28].

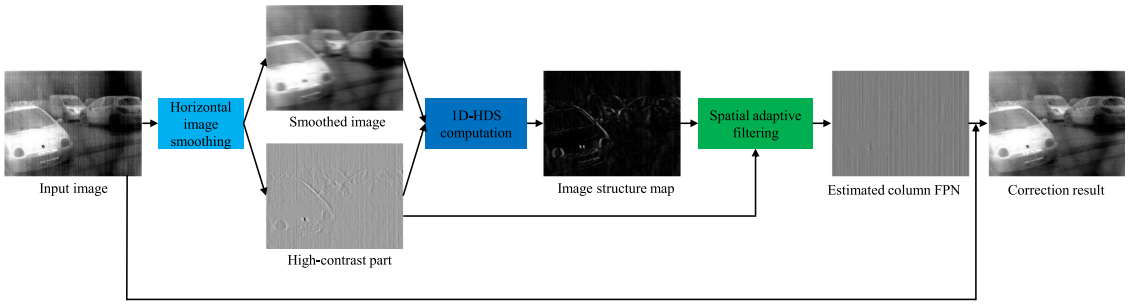

Fig. 2. The workflow of our proposed NUC approach which is able to remove column FPN without losing original image details.

3. Column FPN Correction

In this paper we present a complete image processing workflow to address the problem of column FPN removal for low-textured infrared images. The key idea is to make use of local image variation patterns to separate image structures from column FPN in infrared images, and then apply a spatially adaptive filtering scheme, which behaves differently in structure and non-structure regions, to achieve better performance of noise removal and edge preservation simultaneously. The proposed column FPN correction method consists of three major processing steps. (1) Horizontal image smoothing is applied to divide the input image into a smooth image part and high-contrast signals; (2) 1D Horizontal Differential Statistics are computed to extract major image structures; (3) Noise terms are computed on structure and non-structure regions differently through a spatially adaptive filtering scheme. The computed column FPN is subtracted from the raw input to avoid undesired image blurring effects. The complete processing pipeline is schematically illustrated in Fig. 2.

3.1 Horizontal Image Smoothing

Given a raw infrared image, our method firstly applies 1D horizontal filtering to compute its averaged output. Since image smoothing is only preformed in local horizontal windows, no structure/textures in the vertical direction will get blurred during this processing step. In our implementation, we make use of 1D row guided filter [10], [29] to remove column FPNs while preserving major image structures. This edge-preserving filter uses a variance parameter ϵ to distinguish high-variance edges and low-variance noise. Ideally, only image noise is removed while edges are preserved. However, this strategy does not work well on low-textured infrared images since column FPN is more significant than many thermal details. In our implementation, we set the width of 1D row guided filter to 9 and set the variance parameter to a high value ($\epsilon = 0.4^2$) to completely remove column FPN. The high-contrast components corresponding to image texture and edges are further recovered to avoid undesired image blurring.

As shown in Fig. 3, horizontal image smoothing will divide the raw image $v(i)$ into a smoothed image part $u(i)$ and a horizontal high-frequency component $n(i)$ as:

$$v(i) = u(i) + n(i) = u(i) + s(i) + t(i) \tag{1}$$

It is observed that the extracted high-contrast signal part $n(i)$ contains not only column FPN $s(i)$ but also a significant amount of image original information $t(i)$. As a result, image details are blurred and important thermal targets become unrecognizable in the smoothed output $u(i)$. Since low-textured infrared images only contain a small amount of high-contrast signals (e.g., structural edges and image textures), it is important that true signal component $t(i)$ is further separated from image noise $s(i)$ and added back to $u(i)$ to avoid over-smoothing image.

(a) (b) (c)

Fig. 3. Processing results of 1D horizontal image smoothing. (a) The raw image. (b) The smoothed output. (c) Horizontal high-frequency signals. Note the images are normalized to 0-1 value range for visualization.

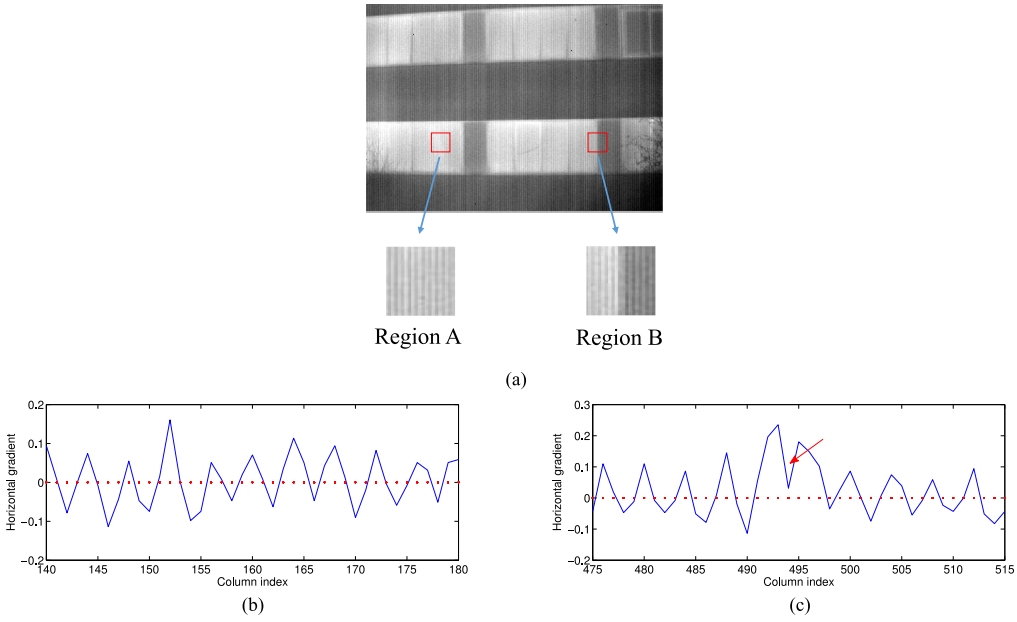

Fig. 4. Structural edges and column FPN will introduce local variations with different patterns. (a) Region A and B are selected in a raw infrared image. (b) Horizontal gradients computed in region A which only contains column FPN. (c) Horizontal gradients computed in region B which also contains a structural edge.

3.2 1D Horizontal Differential Statistics

Although structural edges and column FPN are both high-frequency image signals, they introduce local variations with different patterns. Since column FPN is caused by non-uniformities of column-parallel accumulators and ADCs, it exhibits small-scale oscillations in the horizontal direction and changes from one column to another. Such repetitive image patterns introduce local image variations of similar magnitudes but in different directions. In contrast, a structural edge will break this repetitive pattern and bring in gradients of consistent directions. Some comparative results are shown in Fig. 4. Based on this observation we define a new spatial variation measurement, which is termed as 1D Horizontal Differential Statistics (HDS_{1D}), to capture essential difference between column FPN and structural edges as follows:

$$HDS_{1D}(i) = \left| \frac{1}{K_1(i)} \cdot \sum_{j \in N_h(i)} \exp\left(-\frac{\|u(i) - u(j)\|^2}{2\sigma_{r1}^2} \right) \cdot \partial_x v(j) \right| \tag{2}$$

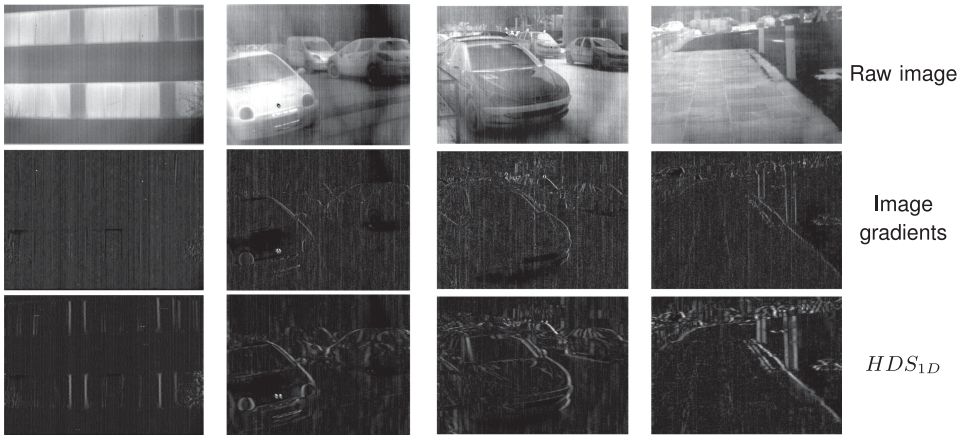

Fig. 5. Comparative results of image vertical structure extraction on raw infrared images which contain obvious column FPN. All images are normalized to 0-1 value range for visualization.

where $K_1(i) = \sum_{j \in N_h(i)} \exp(-\frac{\|u(i)-u(j)\|^2}{2\sigma_{r1}^2})$ is the normalization term, $\partial_x v(j)$ is the computed local gradient in the horizontal direction, $u(i)$ is the output of horizontal image smoothing, $N_h(i)$ is a horizontal window which defines a set of neighboring pixels of i, and σ_{r1} is the range weight parameter. $N_h(i)$ defines how far the kernel will consider the neighbouring pixels to average horizontal gradients. As long as the width of N_h is not set to a very small number (e.g., if we set the width of N_h to 1, the filter won't do averaging at all), the kernel will generate stable averaged output. In our implementation we set the width of N_h to 9. The expression of (2) can be understood as a filter that averages the image gradient $\partial_x v$ guided by the smoothed image $u(i)$. Local gradient $\partial_x v(i)$ and $\partial_x v(j)$ will only be averaged if their corresponding range image $u(i)$ and $u(j)$ are similar. Ideally the range parameter σ_{r1} should be set to the "minimum" amplitude of edges in image u to make pixel i and j are on the same side of a structure edge. In our implementation we fix σ_{r1} to 10× standard deviation of horizontal gradients of image u as suggested in [23]. Note the smoothed image u contains a limited amount of column FPN and structural edges, thus its local image gradients are mostly caused by image noise. Since the value of $\partial_x v(i)$ could be either positive or negative, local gradients in different directions (with different signs) will offset each other. Only gradients in the same direction will be added up to yield large HDS_{1D} values.

Given a raw infrared image containing column FPN, we calculate its 1D Horizontal Differential Statistics based on (2). Note HDS_{1D} values are high for image regions which contain structural components since local significant gradients are also in similar directions. In comparison, HDS_{1D} values are very low in non-structure regions since column FPN introduces gradients of similar magnitudes but in different directions. In such way, HDS_{1D} provides an effective tool to differentiate column FPN and structural edges by exploring their inherent differences. As shown on the second row of Fig. 5, image structures and column FPN cannot be well separated based on image gradients computed at single pixels. In comparison, HDS_{1D} considers pattern information of local variations to successfully extract major vertical structures on raw infrared images as shown on the third row of Fig. 5.

3.3 Spatially Adaptive Filtering

After calculating horizontal high-contrast signal $n(i)$ and 1D Horizontal Differential Statistic $HDS_{1D}(i)$, a new spatially adaptive filtering scheme is proposed to estimate column FPN $s(i)$ as follows:

$$s(i) = \frac{1}{K_2(i)} \sum_{j \in N_v(i)} \exp\left(-\frac{\gamma}{HDS_{1D}(i) + \chi} \cdot \frac{\|i-j\|^2}{2\sigma_{s2}^2}\right) \cdot n(j) \tag{3}$$

(a) (b) (c) (d)

Fig. 6. Processing results using different spatial filtering schemes. (a) Raw image. (b) Correction result using a global model (height of N_v is set to the image height H). (c) Correction result using a local model (height of window N_v is set to $\frac{H}{16}$). (d) Correction result using our proposed spatially adaptive filtering scheme. The proposed method adaptively combines the advantages of global and local-based correction methods and achieves better performance on both eliminating column FPN and preserving image edges. Please zoom in to check details.

where $K_2(i) = \sum_{j \in N_v(i)} \exp(-\frac{\gamma}{HDS_{1D}(i)+\chi} \cdot \frac{\|i-j\|^2}{2\sigma_{s2}^2})$ is for normalization, N_v is a local 1D vertical window in which column FPN correction terms are computed, the threshold parameter γ is set to 0.5 to differentiate structure and non-structure pixels, χ is a small positive number to avoid division by zero, and σ_{s2} is the spatial range parameter. Parameters σ_{s2} and height of N_v in (3) define how many neighbouring pixels to consider for computing column FPN correction terms. In our proposed method, we set σ_{s2} and height of N_v to large values ($\sigma_{s2} = 0.8\times$ image height H and height of $N_v = H$) to impose a global correction model initially. For a pixel with a high $HDS_{1D}(i)$ (corresponding to an image structure), the $\frac{\gamma}{HDS_{1D}(i)+\epsilon}$ term yields a low value. In this situation, information of more neighboring pixels will be considered through a more stable global model and the estimated correction terms can better preserve image original information. For a pixel inside a background patch that only contains column FPN, its corresponding $HDS_{1D}(i)$ is low and the calculated $\frac{\gamma}{HDS_{1D}(i)+\epsilon}$ value is high. The $\frac{\gamma}{HDS_{1D}(i)+\epsilon}$ term will adapt the initial global correction model to a local correction model. Correction terms computed within small vertical windows are more responsive to local variations, thus can better remove column FPN.

In Fig. 6, we show comparative correction results using different spatial filtering schemes. It is observed that local column FPN cannot be accurately compensated by applying a global correction model, while a small fixed-size spatial filtering cannot differentiate strip noise from image textures and its processing results get blurred. In comparison, the spatially adaptive filtering scheme computes noise correction terms in structure and non-structure regions differently. In structure regions, it applies a global correction model to keep image edges, while a local correction model is applied in non-structure regions to eliminate strips. The proposed method adaptively combines the advantages of global and local-based correction methods and achieves better performance on both eliminating column FPN and preserving image details as illustrated in Fig. 6(d).

4. Evaluation Method

Given a ground truth image, *PSNR* is the most commonly used performance indicator of denoising algorithms. As a pre-processing step, NUC is immediately applied on the raw infrared data to remove FPNs thus a noise-free reference image is not available to compute *PSNR*. It is desirable to develop reference-free methods to evaluate NUC techniques. Until now, several single-image based methods, such as roughness index [8], $RMSE_{AP}$ [10], and Energy of Line Gradient [11], have been proposed for performance evaluation of column FPN correction methods. Even though these methods may appear very different in formulas, they share the same basic principle that better column FPN correction method leads to lower horizontal gradients in its output. The major limitation of these methods is that they only characterize how well an algorithm can remove column FPN, but cannot evaluate the ability of this algorithm to keep original image information. For instance, over-smoothing an infrared image will completely eliminate column FPN and produce low horizontal

gradients, but it is not an ideal correction solution since important thermal details get adversely removed as well.

To address the above problem, we propose a new reference-free methodology to evaluate performance of column FPN correction methods. If a column FPN correction method works well, it should remove strip artifacts while preserving structural edges. It means that gradients caused by column FPN and structural edges should be suppressed differently. More specifically, gradients caused by column FPN should decrease as much as possible, while gradients caused by image structures should remain almost unchanged. Based on above considerations, we present a new evaluation method by exploring how differently horizontal gradient suppression is performed in structure and non-structure regions as follows:

$$D_{s_T}^{s_F}(G, v) = \frac{\sum_{i \in s_T} \partial_x G(v(i))}{\sum_{i \in s_T} \partial_x v(i)} - \frac{\sum_{i \in s_F} \partial_x G(v(i))}{\sum_{i \in s_F} \partial_x v(i)} \tag{4}$$

where $v(i)$ is the raw image, $G(.)$ denotes a proposed column FPN correction method, s_T and s_F are pixels in structure and non-structure regions which are defined by referring to the computed HDS_{1D}. A pixel is considered as a structure pixel if its corresponding HDS_{1D} value is higher than a threshold, otherwise it is a non-structure pixel. Since infrared images only contain a limited amount of textures [6], in our implementation we set the threshold to a high value (top 1% of all HDS_{1D} values). Higher $D_{s_T}^{s_F}(G, v)$ value indicates the proposed FPN correction method G has a better ability to remove column FPN while preserving original information. Please note here we investigate whether $D_{s_T}^{s_F}$ of a method is higher than $D_{s_T}^{s_F}$ of another method for the purpose of performance comparison, rather than their absolute $D_{s_T}^{s_F}$ values.

To verify the effectiveness of our proposed evaluation method, we apply it to assess three different column FPN correction methods including 1D Gaussian filtering (Method A), 1D guided filtering (Method B), and our proposed NUC method (Method C). These methods are individually applied to a number of raw infrared images (10 images in total). Fig. 7 shows some processing results of different correction methods. We invited 5 different reviewers to evaluate the FPN correction results based on their visual observations. It is observed that 1D Gaussian filtering is a general image denoising technique which reduces gradients equally within an image without differentiating image edges from column FPN. Important thermal details are blurred and many significant objects become unrecognizable as shown in Fig. 7(b). 1D guided filtering is an edge-preserving denoising method, thus it removes low-variance signals while keeping high-variance ones. It produces better denoising results since it can preserve major image structures. However, still lots of thermal details are removed as shown in Fig. 7(c). In comparison, all 5 reviewers picked our proposed method as the best performing denoising method since it can effectively remove column FPN while preserving image fine details, as illustrated in Fig. 7(d).

For the purpose of comparison, our proposed $D_{s_T}^{s_F}$ and two other reference-free methods, roughness index [8] and $RMSE_{AP}$ [10], are used for performance evaluation. The roughness index (R_{index}) is computed by analyzing the high-pass contents of an image in both horizontal and vertical directions as follows [8]:

$$R_{index} = \frac{\|h_1 * f\|_1 + \|h_2 * f\|_1}{\|f\|_1} \tag{5}$$

where $*$ denotes image convolution, f is the image to evaluate, $h_1 = [-1, 1]$ is a horizontal mask, $h_2 = [-1; 1]$ is a vertical mask, and $\|.\|_1$ denotes the L_1 norm. $RMSE_{AP}$ is also computed as another quantitative performance indicator as follows [10]:

$$RMSE_{AP} = \sqrt{\frac{\sum_{x=1}^{M} \sum_{y=1}^{N-1} (f(x, y) - f(x, y+1))^2}{M \times (N-1)}} \tag{6}$$

where M, N are the height and width of image f, and $f(x, y)$ denotes pixel value on row x and column y. The mean $RMSE_{AP}$, R_{index}, and $D_{s_T}^{s_F}$ of different FPN correction methods are shown in Table 1. It is observed that only the computed $D_{s_T}^{s_F}$ values are consistent with visual observation

(a) (b) (c) (d)

Fig. 7. Some sample results using different column FPN correction methods. (a) Raw images. (b) Correction results using 1D Gaussian filtering. (c) Correction results using 1D guided filtering. (d) Correction results using our proposed method. Please zoom in to check details.

TABLE 1
Evaluation Results of Different NUC Methods

	Method A	Method B	Method C	Best Performer
Mean $RMSE_{AP}$ [10]	**2.277**	3.3396	10.5426	Method A
Mean R_{index} [8]	**0.1451**	0.1574	0.3305	Method A
Mean $D_{s_T}^{s_F}$	0.1458	0.3377	**0.4520**	Method C

Note a better column FPN correction method will generate lower $RMSE_{AP}$ and R_{index} but higher $D_{s_T}^{s_F}$ values.

as $D_{s_T}^{s_F}(A) < D_{s_T}^{s_F}(B) < D_{s_T}^{s_F}(C)$. However, $RMSE_{AP}$ [10] and R_{index} [8] both wrongly indicate Method A (1D Gaussian filtering) is the best performing correction method since the results of Method A contain the lowest image gradients.

(a) (b) (c) (d) (e)

Fig. 8. Some sample images from our testing dataset. It is observed that these images cover a wide range of contents (e.g., vehicle, machine, pedestrian, and building). These infrared images will be made publicly available in the future.

5. Experimental Results

In this section, the proposed NUC technique is thoroughly investigated using realistic infrared images. We make use of some publicly available infrared images under the CC-BY license [3] and some of our own captured infrared images to demonstrate that our method is applicable to images captured by different infrared devices.

We consider a number of state-of-the-art column FPN correction methods for comparison. MHE method [26] assumes that histograms of two adjacent columns are similar, and then performs horizontal column histogram smoothing to correct intensity variances caused by strips. It is one of the best performing column FPN correction solutions and can effectively eliminate strip noise without blurring edges. Its source code is available under the CC-BY license [26]. Previously, Cao *et al.* proposed an improved NUC method based on 1D guided filters (1D-GF) [10]. It delivers better correction performance compared with state-of-the-art 1-D and 2-D denoising techniques [19], [22]–[24], [26]. For its implementation, we set $\epsilon_1 = 0.4^2$ and $w = 9$ for the horizontal edge-preserving filtering step and $\epsilon_2 = 0.2^2$ and $h = \frac{H}{4}$ for the vertical strip noise decomposition step. We also consider a global model based correction solution [19] (L-model). This method firstly computes the averages of the first- and second-order statistics for a number of neighboring columns (in our implementation we make use of information from 9 neighboring columns), and then applies a linear correction model to make adjacent columns have similar statistics.

5.1 Qualitative Evaluation

In total 20 raw infrared images are used for performance evaluation. Fig. 8 shows some sample images. These images cover a wide range of scenes (e.g., indoor and outdoor). Fig. 9 shows some comparative results of our proposed NUC method and three other state-of-the-art solutions [10], [19], [26]. As shown on the second row of Fig. 9, the global model based solution (L-model [19]) does not produce satisfactory FPN correction results. A large amount of strips remain visible in its processing results. It is because locally changed column FPN cannot be effectively compensated using a global correction model. The processing results of MHE-based method and 1D-GF are shown on the third and fourth rows of Fig. 9 respectively. It is observed that some vertical strips are not correctly removed and some small targets (e.g., a vehicle behind a tree highlighted in the first raw image) get lost in the results of MHE method. Another drawback of MHE-based method is that it will falsely generate obvious image artifacts which are problematic for object detection or target recognition in surveillance applications. 1D-GF method accurately decomposes image noise from the extracted high-frequency signals, thus it can better remove column FPN without causing undesired artifacts. However, 1D-GF method is based on fixed-size 1D guided filters and will blur

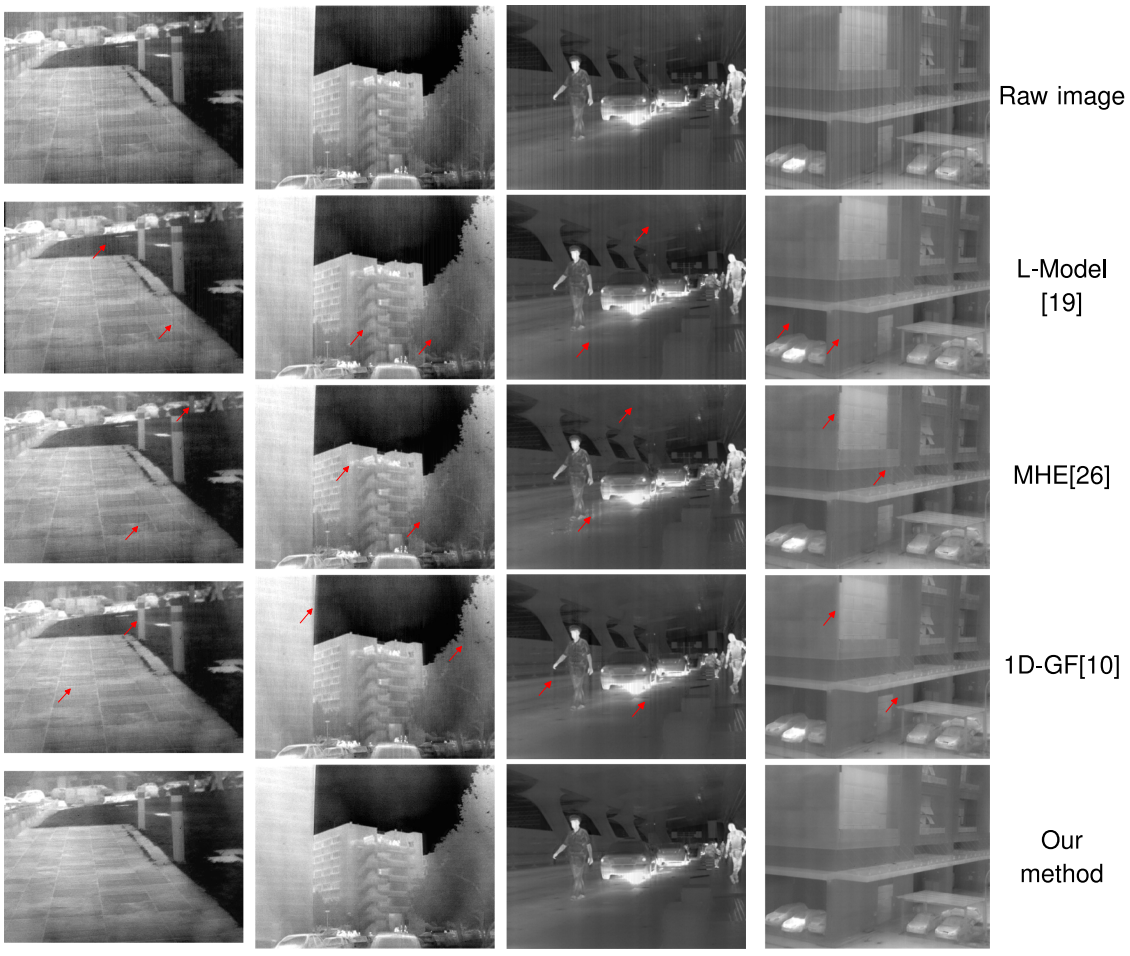

Fig. 9. Some comparative results of our proposed method and three other column FPN correction solutions [10], [19], [26]. The first two raw images are from a publicly available infrared image dataset under the CC-BY license [3] and the third and fourth raw images are our own captured infrared data. Please zoom in to check details highlighted.

some vertical image structures as highlighted in Fig. 9. In comparison, our proposed method applies different noise correction models in structure and non-structure regions through a spatially adaptive filtering scheme. It adaptively combines the advantages of global and local correction methods and achieves better performance on both eliminating column FPN and preserving image details as shown on the last row of Fig. 9.

5.2 Quantitative Evaluation

We compute $D_{S_T}^{S_F}$ and $RMSE_{AP}$ based on (4) and (6) respectively to quantitatively evaluate different column FPN correction solutions. These two evaluation methods provide complementary information on how well a column FPN correction method works. Since differences between adjacent pixels are mostly caused by column FPN, lower $RMSE_{AP}$ value indicates better performance of noise removal. On the other hand, higher $D_{S_T}^{S_F}$ value suggests the proposed FPN correction method has a better ability to preserve original information. The quantitative evaluation results (mean $D_{S_T}^{S_F}$ and mean $RMSE_{AP}$) are shown in Table 2. It is observed that our method yields the lowest $RMSE_{AP}$ and the highest $D_{S_T}^{S_F}$ values for all testing images. The experimental results illustrate that our proposed

TABLE 2
Computed Mean $D_{S_T}^{S_F}$ and $RMSE_{AP}$ of Results Using Different Column FPN Correction Solutions

	Raw image	L-Model [19]	MHE [26]	1D-GF [10]	Our method
Mean $D_{S_T}^{S_F}$	0	0.3742	0.4132	0.3727	**0.4938**
Mean $RMSE_{AP}$ [10]	16.1192	9.8084	9.2552	8.6683	**8.3052**

Note higher $D_{S_T}^{S_F}$ values indicate better ability to differentiate image structures (signals to preserve) from column FPN (signals to remove). In comparison, lower $RMSE_{AP}$ value indicates better performance of noise removal.

method can not only better eliminate strip noise in infrared images but also preserve original image information.

6. Conclusion

Column FPN significantly degrades radiometric accuracy of infrared images captured by uncooled long-wave infrared FPA. In this paper we firstly address the problem of column FPN correction. It is observed that a structural edge will introduce local gradients of consistent orientations while column FPN generates local variations of similar magnitudes but in different directions. With this observation, we define 1D Horizontal Differential Statistics to separate image structures from strip noise. Based on the image structure map, a spatially adaptive filtering scheme is proposed to compute noise terms in structure and non-structure regions using different correction models. The proposed method can effectively eliminate column FPN while preserving other high-frequency signals including major edges and image details. In the second part of this paper, we present a reference-free methodology to evaluate performance of column FPN correction methods. This valuation method provides an effective tool to assess how well an algorithm removes column FPN as well as its ability to preserve image original information. In the future, we plan to implement the proposed NUC method in our hardware device to improve the quality of image data for advanced infrared applications such as target detection, object recognition, and thermal diagnosis.

Acknowledgment

The authors would like to thank Dr. C.-L. Tisse (ULIS, France) for his helpful discussion and Dr. A. Renfrew for his help in proofreading. The authors would also like to thank the handling editor and anonymous reviewers for their valuable suggestions.

References

[1] Z. Liu, J. Xu, X. Wang, K. Nie, and W. Jin, "A fixed-pattern noise correction method based on gray value compensation for TDI CMOS image sensor," *Sensors*, vol. 15, no. 9, pp. 23496–23513, 2015.
[2] X. Sui, Q. Chen, and G. Gu, "Adaptive grayscale adjustment-based stripe noise removal method of single image," *Infrared Phys. Technol.*, vol. 60, pp. 121–128, 2013.
[3] Y. Tendero and J. Gilles, "Admire: A locally adaptive single-image, non-uniformity correction and denoising algorithm: application to uncooled IR camera," *Proc. SPIE*, vol. 8353, 2012, Art. no. 83531O.
[4] C. Tomasi and R. Manduchi, "Bilateral filtering for gray and color images," in *Proc. 6th Int. Conf. Comput. Vis.*, 1998, pp. 839–846.
[5] K. He, J. Sun, and X. Tang, "Guided image filtering," *IEEE Trans. Pattern Anal. Mach. Intell.*, vol. 35, no. 6, pp. 1397–1409, Jun. 2013.
[6] N. J. Morris, S. Avidan, W. Matusik, and H. Pfister, "Statistics of infrared images," in *Proc. IEEE Conf. Comput. Vis. Pattern Recognit.*, 2007, pp. 1–7.

[7] D. C. Adler, T. H. Ko, and J. G. Fujimoto, "Speckle reduction in optical coherence tomography images by use of a spatially adaptive wavelet filter," *Opt. Lett.*, vol. 29, no. 24, pp. 2878–2880, 2004.
[8] L. Rui, Y. Yin-Tang, L. Qing, and Z. Hui-Xin, "Improvement in adaptive nonuniformity correction method with nonlinear model for infrared focal plane arrays," *Opt. Commun.*, vol. 282, no. 17, pp. 3444–3447, 2009.
[9] J. Zhao *et al.*, "Single image stripe nonuniformity correction with gradient-constrained optimization model for infrared focal plane arrays," *Opt. Commun.*, vol. 296, pp. 47–52, 2013.
[10] Y. Cao, M. Y. Yang, and C.-L. Tisse, "Effective strip noise removal for low-textured infrared images based on 1-D guided filtering," *IEEE Trans. Circuits Syst. Video Technol.*, vol. 26, no. 12, pp. 2176–2188, Dec. 2016.
[11] W. Qian, Q. Chen, G. Gu, and Z. Guan, "Correction method for stripe nonuniformity," *Appl. Opt.*, vol. 49, no. 10, pp. 1764–1773, 2010.
[12] D. L. Perry and E. L. Dereniak, "Linear theory of nonuniformity correction in infrared staring sensors," *Opt. Eng.*, vol. 32, no. 8, pp. 1854–1859, 1993.
[13] D. R. Pipa, E. A. da Silva, C. L. Pagliari, and P. S. Diniz, "Recursive algorithms for bias and gain nonuniformity correction in infrared videos," *IEEE Trans. Image Process.*, vol. 21, no. 12, pp. 4758–4769, Dec. 2012.
[14] M. Maggioni, E. Snchez-Monge, and A. Foi, "Joint removal of random and fixed-pattern noise through spatiotemporal video filtering," *IEEE Trans. Image Process.*, vol. 23, no. 10, pp. 4282–4296, Oct. 2014.
[15] J. G. Harris and Y.-M. Chiang, "Nonuniformity correction of infrared image sequences using the constant-statistics constraint," *IEEE Trans. Image Process.*, vol. 8, no. 8, pp. 1148–1151, Aug. 1999.
[16] E. Vera, P. Meza, and S. Torres, "Total variation approach for adaptive nonuniformity correction in focal-plane arrays," *Opt. Lett.*, vol. 36, no. 2, pp. 172–174, 2011.
[17] R. C. Hardie, M. M. Hayat, E. Armstrong, and B. Yasuda, "Scene-based nonuniformity correction with video sequences and registration," *Appl. Opt.*, vol. 39, no. 8, pp. 1241–1250, 2000.
[18] J. Zeng, X. Sui, and H. Gao, "Adaptive image-registration-based nonuniformity correction algorithm with ghost artifacts eliminating for infrared focal plane arrays," *IEEE Photon. J.*, vol. 7, no. 5, Oct. 2015, Art. no. 6803016.
[19] B. Narayanan, R. C. Hardie, and R. A. Muse, "Scene-based nonuniformity correction technique that exploits knowledge of the focal-plane array readout architecture," *Appl. Opt.*, vol. 44, no. 17, pp. 3482–3491, 2005.
[20] L. Liu and T. Zhang, "Optics temperature-dependent nonuniformity correction via ℓ_0-regularized prior for airborne infrared imaging systems," *IEEE Photon. J.*, vol. 8, no. 5, Oct. 2016, Art. no. 3900810.
[21] Y. Cao and C.-L. Tisse, "Single-image-based solution for optics temperature-dependent nonuniformity correction in an uncooled long-wave infrared camera," *Opt. Lett.*, vol. 39, no. 3, pp. 646–648, 2014.
[22] K. He, J. Sun, and X. Tang, "Guided image filtering," in *Computer Vision–ECCV 2010*. New York, NY, USA: Springer, 2010, pp. 1–14.
[23] A. Buades, B. Coll, and J.-M. Morel, "A non-local algorithm for image denoising," in *Proc. IEEE Comput. Soc. Conf. Comput. Vis. Pattern Recognit.*, 2005, vol. 2. IEEE, pp. 60–65.
[24] K. Dabov, A. Foi, V. Katkovnik, and K. Egiazarian, "Image denoising by sparse 3-D transform-domain collaborative filtering," *IEEE Trans. Image Process.*, vol. 16, no. 8, pp. 2080–2095, Aug. 2007.
[25] X.-B. Sui, Q. Chen, and G.-H. Gu, "Algorithm for eliminating stripe noise in infrared image," *J. Infrared Millimeter Waves*, vol. 31, no. 2, pp. 106–112, 2012.
[26] Y. Tendero, S. Landeau, and J. Gilles, "Non-uniformity correction of infrared images by midway equalization," *Image Process. Line*, vol. 2012, pp. 134–146, 2012.
[27] Y. Chang, H. Fang, L. Yan, and H. Liu, "Robust destriping method with unidirectional total variation and framelet regularization," *Opt. Exp.*, vol. 21, no. 20, pp. 23307–23323, 2013.
[28] Q. Zhang, X. Shen, L. Xu, and J. Jia, "Rolling guidance filter," in *Proc. Eur. Conf. Comput. Vis.*, 2014, pp. 815–830.
[29] K. Ohata *et al.*, "Hardware-oriented stereo vision algorithm based on 1-D guided filtering and its FPGA implementation," in *Proc. IEEE 20th Int. Conf. Electron., Circuits, Syst.*, 2013, pp. 169–172.